Role of hyperthermia in overcoming HPV-mediated MHC-I downregulation and promoting immune surveillance

HANYU WANG[1,2*], HONGXIN LANG[3*], YAOXING GUO[1,2], TE SUN[1,2], YUANSONG BAI[4], TAO ZHANG[3] and RUI-QUN QI[1,2]

[1]Department of Dermatology, The First Hospital of China Medical University, Shenyang, Liaoning 110001, P.R. China; [2]Key Laboratory of Immunodermatology, Ministry of Education and National Health Commission of the People's Republic of China, National Joint Engineering Research Center for Theranostics of Immunological Skin Diseases, Shenyang, Liaoning 110001, P.R. China; [3]Department of Stem Cell and Regenerative Medicine, College of Basic Medicine, Shenyang Key Laboratory of Stem Cell and Regenerative Medicine, China Medical University, Shenyang, Liaoning 110122, P.R. China; [4]Department of Environmental Stress Research, School of Public Health, China Medical University, Shenyang, Liaoning 110122, P.R. China

Received December 10, 2025; Accepted June 16, 2026

DOI: 10.3892/ijmm.2026.5924

Abstract. Immune-regulatory dysfunction caused by human papillomavirus (HPV) infection can lead to severe condyloma acuminate (CA), and the treatment is challenged by obstinacy and recurrence. Hyperthermia treatment stimulates the immune response by raising the body temperature locally to fight pathogens. Hyperthermia treatment possesses advantages of low recurrence rate and good efficacy in curing viral warts. However, the exact modulatory mechanism of hyperthermia treatment on immune response remains to be addressed. HPV 16 pseudovirus (HPV.PSV)-infected HaCaT cells were established to mimic clinical HPV infection. Flow cytometry showed higher major histocompatibility complex class I (MHC-I) expression in HPV.PSV infected cells. HPV.PSV-infected cells, CaSki cells and CA tissue demonstrated upregulated MHC-I expression following 44˚C water bath incubation, as detected by flow cytometry and IHC. 4D-FastDIA quantitative proteomics was used to analyze differential protein expression in CaSki cells following 37- or 44˚C incubation. High mobility group box (HMGB)1 was upregulated following 44˚C incubation, as shown by ELISA and western blotting. By applying HMGB1 knockdown cell lines established by small interfering RNA, the present study demonstrated HMGB1 was essential to MHC-I expression, which was detected by flow cytometry and the recombinant HMGB1 protein addition test. Western blotting and ELISA demonstrated that hyperthermia increased heat shock protein family A member 6 (HSPA6) expression and JNK phosphorylation, which resulted in greater secretion of HMGB1. Hyperthermia treatment facilitated HSPA6-modulated JNK phosphorylation, which lead to HMGB1 secretion and enhanced the expression of MHC-I in HPV-infected epithelial cells, as well as strengthened the host immune regulation and recognition.

Correspondence to: Professor Rui-Qun Qi, Department of Dermatology, The First Hospital of China Medical University, 155 Nanjing North Street, Heping, Shenyang, Liaoning 110001, P.R. China
E-mail: xiaoqiliumin@163.com

Professor Tao Zhang, Department of Stem Cell and Regenerative Medicine, College of Basic Medicine, Shenyang Key Laboratory of Stem Cell and Regenerative Medicine, China Medical University, 77 Puhe Road, Shenbei, Shenyang, Liaoning 110122, P.R. China
E-mail: cmuzhangtao@163.com

*Contributed equally

Key words: hyperthermia treatment, MHC-I, HMGB1, human papillomavirus, JNK

Introduction

Human papillomavirus (HPV) is a sexually transmitted virus with high contagion. It is a non-enveloped DNA virus and there are >400 genotypes (1). HPV infection induces immune escape by suppressing host immune surveillance system, resulting in decreased effectiveness of antigen presentation and immune response (2). Existing vaccines prevent partial HPV infection, but patients with condyloma acuminate (CA) typically experience refractory recurrence (3). HPV is classified into low-(mainly including HPV 6 and 11) and high-risk (mainly including HPV 16 and 18) groups. High-risk HPVs are associated with oncogenesis and CA which is a sexually transmitted disease affecting the genitals, anus and surrounding area (4,5). HPV 16 and 18 cause >70% of cervical cancers (6). More than half of healthy individuals show the presence of high-risk HPV types in CA lesions, including HPV 16, 18, 55 and 59 (7). Consequently, management must address not only the removal of warts but also the reduction of potential oncogenesis risk from high-risk HPV.

Hyperthermia treatment is applied in multiple immune disorders as an immunoregulatory method (8,9). Hyperthermia is typically induced *in vitro* via 44˚C water

bath incubation (10-17). Hyperthermia treatment is efficient in treating viral warts clinically (12). Infrared hyperthermia treatment is used in clinical therapy with high efficiency and low recurrence and can enhance immune recognition and immune activation via inducing local hyperthermia (18). Hyperthermia treatment can facilitate tissue repair, immunoefficacy and immune surveillance (18,19). Hyperthermia treatment decreases the expression of CCL-20 with concomitant decrease in IL-1α, and decreases the number of Langerhans cells in HPV-infected skin (20). Meanwhile, hyperthermia decreases HaCaT cell proliferation and promotes cytokine expression, which is responsible for anti-viral activity, through a NF-κB-dependent pathway (15). Local hyperthermia combined with imiquimod clears recalcitrant and extensive warts in patients with systemic lupus erythematosus (21). However, how hyperthermia treatment regulates immune surveillance function remains elusive.

Although hyperthermia elevates major histocompatibility complex class I (MHC-I) expression in tumor cells, its role during HPV infection remains unclear (22). MHC-I is an essential regulator during immune evasion and serves a key role in antigen presentation (23). MHC-I presents endogenous antigen peptides to the cell surface; binding to T cell receptors activates $CD8^+$ T cells and triggers the immune response (24). MHC-I-mediated antigen recognition induces the proliferation and differentiation of cytotoxic T lymphocytes (CTLs), which directly participates in the death of virus-infected and tumor cells (23,25). HPV infection inhibits expression of MHC-I on host cells, and leads to escape from immune surveillance and persistent infection (26,27). Increased expression of MHC-I is considered as an effective way to strengthen immune response of HPV-induced diseases (27-29). The present study aimed to reveal whether hyperthermia treatment can treat HPV infection through regulating MHC-I-mediated immunological recognition.

High mobility group box (HMGB)1 is a DNA-binding protein but not a histone (30). HMGB1 is categorized as a damage-associated molecular pattern (DAMP) member and is associated with inflammatory disorders among numerous types of tumor, such as non-small cell lung, colon and breast cancer, liver hepatocellular carcinoma (31-35). HMGB1 is an intracellular signal involved in immune regulation and cellular stress through regulating gene transcription and chromatin structure (36,37). HMGB1 undergoes extracellular secretion following stimulation and damage sensing, then activates innate and acquired immune responses (38). It is reported that JNK pathway signaling modulates external secretion of HMGB1 (39). In idiopathic inflammatory myopathy, as an early pro-inflammatory molecule, HMGB1 induces high expression of MHC-I on muscle fibers via autocrine and paracrine pathways, which results in a pro-inflammatory microenvironment (40). The neutralization of HMGB1 downregulates the expression of MHC-I in muscle tissue of mice with idiopathic inflammatory myopathy, and decreases inflammatory cytokines infiltration (41). Therefore, hyperthermia may serve as an advantageous stimulating signal to drive HMGB1 secretion and activate immune response locally.

Although studies have proven that hyperthermia regulates the immune response (42-45), it remains unclear how hyperthermia treats HPV infection. To mimic CA, the present study used HPV 16 pseudovirus (HPV.PSV)-infected HaCaT cells and HPV-positive CaSki cells to analyze the regulatory role of hyperthermia and its role in MHC-I-related immune regulation.

Materials and methods

HPV.PSV preparation. HPV.PSV was synthesized by Sangon Biotech Co., Ltd. Briefly, the chemical synthetic HPV16 gene sequence (NCBI accession no. LC511112.1) was cloned and constructed into adeno-associated virus vector. The constructed vector was transfected into 293 cells for packaging and preparation of PSV. The samples were purified by chromatographic columns to remove cell debris and impurities, and concentrated by ultracentrifugation to obtain high concentration of HPV.PSV. The detailed procedures for pseudovirus synthesis, chromatography and ultracentrifugation are not publicly available.

Cell culture and HSP.PSV infection. HaCaT (cat. no. SCSP-5091) and CaSki (cat. no. TCHu137) cells were purchased from Cell Bank, Chinese Academy of Sciences. HaCaT cells were authenticated by STR profile analysis by Genetic Testing Biotechnology Corporation (Suzhou, China). HaCaT cells were cultured with DMEM, 10% FBS (both Procell Life Science & Technology Co., Ltd.) and 1% penicillin-streptomycin at 37˚C in a 5% CO_2 incubator. CaSki cells were cultured with RPMI 1640 (Procell Life Science & Technology Co., Ltd.), 10% FBS, and 1% penicillin-streptomycin at 37˚C in a 5% CO_2 incubator. HaCaT cells were seeded in a 6-well plate at a density of 70% and treated with HPV.PSV at 100 MOI for 24 h at 37˚C. To assess infection efficiency, reverse transcription-quantitative (RT-q)PCR was used to evaluate the HPV16 mRNA expression between HaCaT cells transfected with HPV.PSV and control virus.

Cell treatment with rHMGB1. HaCaT and CaSki cells were seeded into 6-cm cell culture dishes until reached a density of 70% at 37˚C, then the culture medium was replaced with fresh medium. The lyophilized powder of rHMGB1 (MCE, cat. no. HY-P70274, protein-human-hek-293-his.html) was dissolved in sterile PBS buffer. Cells were treated with rHMGB1 at a final concentration of 200 ng/ml at 37˚C for 12 h, while control cells received an equal volume of sterile PBS buffer.

Hyperthermia treatment. HPV.PSV-infected HaCaT and CaSki cells were incubated at 37 or 44˚C in a water bath for 30 min. A 30-min treatment in a 44˚C water bath is a standardized *in vitro* treatment protocol in thermal therapy research (46). All samples were put back in a 37˚C, 5% CO_2 incubator after treatment. The cells were recovered for 12 h at 37˚C.

Clinical samples collecting. In total, nine skin warty samples from patients with CA were collected between February 2023 and February 2024 from the Department of Dermatology, The First Affiliated Hospital of China Medical University, Shenyang, China. Written informed consent was obtained from all patients prior to enrollment in this study. All procedures were approved by Hospital Medical Science Research

Ethics Committee of the First Affiliated Hospital of China Medical University [approval no. (2023)214]. The inclusion criteria were as follows: i) Patients with CA aged 18-60 years; ii) no other concurrent sexually transmitted diseases (such as gonorrhea, syphilis); and iii) no other concurrent systemic disease (such as malignant tumors, autoimmune diseases). The exclusion criteria were as follows: i) Topical medication within the previous 2 weeks; ii) treatment with glucocorticoids or immunosuppressants within the previous 1 month; iii) other sexually transmitted diseases (such as gonorrhea, syphilis); and iv) systemic diseases (such as malignant tumors, autoimmune disease). The patients included five females and four males, with an age range of 19-35 years. The lesion sites were distributed as follows: Vulva (5 cases), penile coronal sulcus (3 cases) and groin (1 case).

Samples were preserved in pre-cooled RPMI-1640 and treated in a water bath as aforementioned.

Flow cytometry. Cultured HaCaT and CaSki cells were digested with trypsin and washed by pre-cooled PBS. In total, $1x10^7$ cells were harvested for flow cytometry. Cells were resuspended in binding buffer and incubated with anti-MHC-I-FITC (1:1,000, Elabscience; Elabscience Bionovation, Inc.; cat. no. E-AB-F1130L) for 30 min in the dark at 4˚C. After washing with binding buffer, cells underwent detection by flow cytometer (BD FACSymphony A1, BD Biosciences). The flow cytometry data was analyzed by FlowJo (v10.8, BD Biosciences). Mean fluorescence intensity was used to compare MHC-I expression.

4D-FastDIA quantitative proteomics. In total, 2 μl supernatant from CaSki cells underwent 4D-FastDIA quantitative proteomics analysis, performed by PTM Biolabs, Inc. For mass spectrometry (MS) and proteomics, the tryptic peptides were dissolved in solvent A, directly loaded onto a reversed-phase analytical column (25 cm length, 100 μm inner diameter). The mobile phase consisted of solvent A (0.1% formic acid, 2% acetonitrile in water) and solvent B (0.1% formic acid in acetonitrile). Peptides were separated with following gradient: 0-13 min, 6-24% B; 14-15 min, 24-35% B; 16-17 min, 35-80% B; 18-20 min, 80% B, all at a constant flow rate of 500 nl/min on a NanoElute UHPLC system (Bruker Daltonics). The peptides were subjected to capillary source followed by the timsTOF Pro 2 MS (Bruker, cat. no. tims TOF PRO 2). The electrospray voltage was 1.75 kV. Precursors and fragments were analyzed at the time of flight detector. The timsTOF Pro was operated in data independent parallel accumulation serial fragmentation (DIA-PASEF) mode. The full scan was set at 300-1,500 m/z with 20PASEF-mode MS/MS scans included in each acquisition cycle. The MS/MS scan range was 400-850 m/z and isolation window was 7 m/z. The DIA data were processed using DIA-NN search engine (v.1.8) (github.com/vdemichev/DiaNN) (47). MS/MS were searched against Homo_sapiens_9606_SP_20231220.fasta (20,429 entries; uniprot.org/) concatenated with reverse decoy database. Trypsin/P was specified as cleavage enzyme allowing up to 1 missing cleavages. Excision on N-term Met and carbamidomethyl on Cys were specified as fixed modification. False discovery rate was adjusted to <1%.

The analysis was based on the raw files obtained from MS. First, a specific protein database was constructed according to the sample origins. Quality control of the proteins and peptide segments was based on the database retrieval. Protein quantitative analysis was performed, covering quantitative distribution and repeatability assessment. The identified proteins underwent functional annotation using Gene Ontology (geneontology.org/), Kyoto Encyclopedia of Genes and Genomes (kegg.jp/), Search Tool for the Retrieval of Interacting Genes/Proteins (string-db.org/) and Clusters of Orthologous Groups/Eukaryotic Orthologous Groups, ncbi.nlm.nih.gov/research/cog/). Protein domains were analyzed by UniProt (uniprot.org/). Differential expression proteins were screened based on log2|fold-change|>1.2 and P-value <0.05. A heat map was constructed by GraphPad Prism 8.0 (Dotmatics) to show the top ranking differently expressed proteins.

RT-qPCR. Cells were washed with PBS and added with TransZol Up. RT was performed using RT kit (StarScript III; cat. no. A240) and 2X RealStar universal SYBR qPCR Mix (both Beijing Kangrun Chengye Biotechnology Co., Ltd.; cat. no. A308), according to the manufacturer's instructions. The primer sequences were shown in Table I. *GAPDH* was used as the endogenous reference genes. Applied Biosystems QuantStudio 1 (Thermo Fisher Scientific, Inc.) was used to complete the RT-qPCR detection. The thermocycling conditions were as follows: Initial denaturation at 95˚C for 2 min, followed by 40 cycles of denaturation at 95˚C for 15 sec, annealing at 60˚C for 30 sec and extension at 72˚C for 30 sec. The $2^{-\Delta\Delta Cq}$ method was used to calculate the differential expression (48). The primers were synthesized by Sangon Biotech Co., Ltd. (Table I).

Western blotting. Total cell protein was extracted with total protein extraction kit (cat.no. cat. no. PC101, Epizyme). Cell nuclear and cytoplasmic protein was extracted with protein extraction kit (cat. no. P0028, Beyotime Biotechnology), according to the manufacturer's instructions. BCA method was used for protein quantification. Protein was loaded (20 μg/lane) in 10% SDS-PAGE, and transferred to the 0.45 μm polyvinylidene fluoride membrane. After blocking non-specific binding sites with 5% non-fat milk for 1 h at room temperature, samples were incubated with primary antibodies at 4˚C overnight. Primary antibodies were as follows: Anti-MHC-I (cat. no. 66013-1-Ig), anti-HMGB1 (cat. no. 10829-1-AP), anti-tapasin (cat. no. 30500-1-AP), anti-chromosome region maintenance 1 (CRM1; cat. no. 66763-1-Ig), anti-JNK (all Proteintech Group, Inc.; cat. no. 24164-1-AP), anti-phosphorylated (p-)JNK (Cell Signaling Technology, Inc.; cat. no. 4668T), anti-heat shock protein (HSP)A6 (all 1:1,000, cat. no. 13616-1-AP), anti-GAPDH (both Proteintech Group, Inc.; cat. no. 10494-1-AP), anti-β-tubulin (marker of cytoplasmic protein; both 1:10,000, Selleck Chemicals; cat. no. F0167) (49) and anti-Laminb1 (marker of nuclear proteins; 1:1,000, PTM Bio, cat. no. PTM-5495) (50). Membranes were incubated with HRP-conjugated Goat anti-Mouse (cat. no. SA00001-1) and HRP-conjugated Goat anti-Rabbit (both 1:10,000, Proteintech Group, Inc.; cat. no. SA00001-2) for 1 h at room temperature. Membranes were visualized with enhanced

Table I. Primer and siRNA sequences.

Name	Sequence, 5'→3'
HPV16-Forward	GGAACACTGGGGCAAAGGAT
HPV16-Reverse	AGTCCATAGCACCAAAGCCA
HSPA6-Forward	GCGCAACGTGCTCATTTTTG
HSPA6-Reverse	ACACCAGCGTCAATGGAGAG
HMGB1-Forward	CCTAAGAAGCCGAGAGGCAA
HMGB1-Reverse	AAGTTGACAGAAGCATCCGGG
GAPDH-Forward	AAGAGCACAAGAGGAAGAGAGAGAC
GAPDH-Reverse	GTCTACATGGCAACTGTGAGGAG
si-HMGB1-1-Forward	CCCAGAUGCUUCAGUCAACUUTT
si-HMGB1-1-Reverse	AAGUUGACUGAAGCAUCUGGGTT
si-HMGB1-2-Forward	CAAGGCCCGUUAUGAAAGATT
si-HMGB1-2-Reverse	UCUUUCAUAACGGGCCUUGTT
si-HMGB1-3-Forward	CCUGUCCAUUGGUGAUGUUTT
si-HMGB1-3-Reverse	AACAUCACCAAUGGACAGGTT
si-NC-Forward	UUCUCCGAACGUGUCACGUdTdT
si-NC-Reverse	ACGUGACACGUUCGGAGAAdTdT

dT, deoxythymidine; HPV, human papillomavirus; HMGB, high mobility group box; si, small interfering; NG, negative control.

chemiluminescence horseradish peroxidase substrate kit (cat no. 180-501), and detected by using a Tanon 5200 system (both Tanon Science and Technology Co., Ltd.) Densitometry of the protein bands was quantified using ImageJ software (version 1.53e, National Institutes of Health).

Co-immunoprecipitation (co-IP). Cells were lysed in NP-40 buffer (Beyotime Biotechnology; cat. no. P0013F). Lysates (500 μl) were incubated overnight at 4˚C with 2 μg anti-HSPA6 antibody (cat. no. LS-C816530, LifeSpan Biosciences, Inc.) or control IgG (cat. no. HY-P73904, MedChemExpress), followed by incubation with 20 μl magnetic protein A/G beads (Beyotime Biotechnology; cat. no. P2108) for 2 h at room temperature. Beads were washed three times with 1X TBS and binding proteins were eluted by boiling in 1xSDS loading buffer, then placed on the magnetic rack and let it separate for 1 min and detected by western blotting, as aforementioned.

Immunohistochemistry. Harvested hyperthermia-treated skin tissues were fixed in 4% paraformaldehyde at 4˚C for 24 h. The tissues underwent dehydration, embedded in paraffin wax and sectioned at 4-μm thick. Sections were deparaffinized in xylene and rehydrated through a descending ethanol series for 5 min each, and finally rinsed with distilled water for 5 min. A pressure cooker was used for antigen retrieval for 2 min at 121˚C before reheating to room temperature for 30 min. The sections were washed with PBS 3 times, 5 min each. The staining procedure was performed using Immunohistochemistry UltraSensitive kit (Fuzhou Maixin Biotechnology Development Co., Ltd., cat. no. KIT-9710) according to the manufacturer's instructions. Briefly, the sections were incubated with endogenous peroxidase inhibitor and non-specific staining blocking buffer for 10 min at room temperature. The sections were incubated with primary anti-MHC-I (1:200, Proteintech Group, Inc.; cat. no. 66013-1-Ig) at 4˚C overnight. The sections were washed three times in PBS (5 min each), then incubated with biotin-labeled goat anti-rabbit IgG polymers and streptavidin-peroxidase for 10 min at room temperature. The sections were incubated with DAB and counterstained with hematoxylin for 5 min at room temperature. Finally, the sections were dehydrated through graded ethanol and sealed with neutral resin. The stained sections were imaged with a light microscope (high-resolution panoramic imaging system, Leica GmbH). Analysis was performed using ImageJ software (version 1.53e, National Institutes of Health).

ELISA. Cells were preprocessed with JNK pathway inhibitor SP600125 (cat. no. S1460, Selleck Chemicals): HaCaT cells were pretreated with 20 μM for 30 min and CaSki cells were treated with 10 μM for 24 h at 37˚C. HaCaT cells were treated with 0.5 μM anisomycin and CaSki cells with 5 μM for 24 h at 37˚C. The cells were treated in 37 or 44˚C water bath for 30 min. Supernatant was collected for ELISA. The supernatant was centrifuged for 15 min at 4˚C and 1,000 x g to remove cell debris. HMGB1 secretion was detected using a commercial kit (cat. no. CSB-E08223h, Cusabio Technology, LLC) according to the manufacturer's instructions.

Short hairpin (sh)RNA transfection. HSPA6 shRNA (5'-CAGCAGTTGTGGCACTCAAGC-3') and negative control shRNA (5'-TTCTCCGAACGTGTCACGT-3') were synthesized by Shanghai GeneChem Co., Ltd. The lentiviral vectors for shRNA/negative control were constructed based on the GV493 vector. The lentiviral transfer vector GV493, packaging plasmid pHelper 1.0, and the envelope plasmid pHelper 2.0 were obtained from GeneChem Co., Ltd., with an empty vector used as a negative control. A 2nd-generation self-inactivating lentiviral packaging system was used, and viral particles were produced in 293T cells (Genechem Co.,

Ltd.). For transfection of cells in a 10-cm dish, 20 μg of GV493 transfer vector, 15 μg of pHelper 1.0, and 10 μg of pHelper 2.0 were mixed at a ratio of 4:3:2 and incubated with the cells at 37˚C for 6 h, after which the medium was replaced and viral supernatants were harvested 48-72 h later. For transduction, target cells were incubated with the lentivirus at 37˚C for 24 h, after which the virus-containing medium was replaced with fresh complete medium. 4X10^5 HaCaT and CaSki cells were cultured in 6-well plates at a density of 70% for transfection. shRNA was transfected by HitransG P viral infection reagent (Shanghai GeneChem Co., Ltd.; cat. no. REVG005) according to the manufacturer's instruction. MOI of HaCaT was set as 20, and 10 for CaSki cells. When cell confluence reached >50%, puromycin (2 μg/ml) was added for selection, and the cells were cultured for 2-4 weeks at 37˚C to completely eliminate untransfected cells. The transfection efficiency was detected by RT-qPCR after 72 h incubation, as aforementioned. Stable cells were maintained with puromycin at a concentration of 1 μg/ml.

Small interfering (si)RNA transfection. In total, 4x10^5 HaCaT and CaSki cells were planted in 6-well plates for 24 h at 37˚C and reached a density of 70% before transfection. Culture medium was replaced with antibiotic-free culture medium. siRNA (Table I) was synthesized by Hippo Biotechnology Co., Ltd. and transfected using Lipo8000 at a final concentration of 100 pmol at 37˚C. Fresh complete medium was added 6 h later. The cells were cultured continuously until harvested to validate the interference efficiency at 48 h by RT-qPCR and 72 h by western blot detection, as aforementioned. Based on the interference efficiency, si-HMGB1-1 was used for subsequent experiments.

Cell Counting Kit-8 (CCK8) assay. HaCaT and CaSki cells were seeded in 96-well plates at a density of 8x10^3 cells/well) in 100 μl medium and incubated overnight at 37˚C in a 5% CO_2 incubator. A total of 10 μl CCK8 solution [Seven Innovation (Beijing) Biotechnology Co., Ltd.; cat. no. SC119] was added to each well and the plates were incubated for 1 h at 37˚C. The absorbance was then measured at 450 nm using a microplate reader and cell viability was calculated.

Statistical analysis. GraphPad Prism 8.0 (Dotmatics) was used for statistical analysis. ImageJ1 (National Institutes of Health) was used for semi-quantitative analysis. The unpaired Student's t-test was used for analysis between two groups. One-way ANOVA followed by Tukey's HSD post hoc test was used to compare >2 groups. All data are presented as the mean ± SD of ≥3 independent experimental repeats. $P<0.05$ was considered to indicate a statistically significant difference.

Results

HPV infection decreases the expression of MHC-I. The present study used HPV.PSV infected HaCaT cells to determine the role of hyperthermia treatment in patients with CA. As shown by RT-qPCR, HPV.PSV successfully infected HaCaT cells (Fig. 1A). The presented study aimed to detect the influence of hyperthermia treatment on the expression of MHC-I in infected cells. Western blotting showed that the expression of MHC-I was remarkably downregulated compared with wild-type cells (Fig. 1B). In addition, flow cytometry demonstrated HPV.PSV-infected HaCaT cells exhibited lower expression of MHC-I (Fig. 1C). The data confirmed that the present study successfully established HPV.PSV-infected cells.

Hyperthermia enhances expression of MHC-I on HPV-infected cells and CA tissue. To analyze the regulatory role of hyperthermia on MHC-I expression, HPV.PSV-infected HaCaT cells were incubated in a 44˚C water bath for 30 min. Expression of MHC-I reached a peak at 12 h post-incubation (Fig. 2A). Flow cytometry revealed that MHC-I was significantly elevated in HPV.PSV-infected HaCaT cells at 12 h post-hyperthermia treatment (Fig. 2B). Flow cytometry demonstrated that hyperthermia increased the expression of MHC-I in CaSki cells (Fig. 2C). Hyperthermia-treated samples from patients with CA expressed higher levels of MHC-I than 37˚C-treated samples (Fig. 2D). Hyperthermia treatment increased the expression of MHC-I in HPV-infected epithelial cells and CA tissue.

Hyperthermia induces the expression of HMGB1. To determine the detailed regulatory association between hyperthermia and MHC-I, 4D-FastDIA quantitative proteomics was performed to analyze the differently expressed proteins. The heat map demonstrated the top 21 upregulated proteins in supernatant of 44˚C-treated CaSki cells (Fig. 3A). Among them, HMGB1 activates innate immunity and strengthens adaptive response via TLR4/RAGE as a DAMP and participates in multiple immune-related disorders (51). Additionally, the present results showed time-course induction of HMGB1 following hyperthermia (Fig. 3B). Secretion of HMGB1 reached a peak at 12 h post-treatment, which was consistent with the dynamic expression of MHC-I. The present study detected the secretion of HMGB1 in hyperthermia treated HPV.PSV-infected HaCaT and CaSki cells (Fig. 3C). In CaSki cells, HMGB1 secretion increased by almost 2.5-fold in the hyperthermia-treated group compared with the control group (Fig. 3C). HMGB1 is secreted by a cytoplasmic transport pathway (52). The present study analyzed the expression of HMGB1 in nuclear and cytosolic protein. Both in HPV.PSV-infected HaCaT and CaSki cells, hyperthermia promoted HMGB1 translocation from nucleus to the cytosol (Fig. 3D and E). Hyperthermia promoted the secretion of HMGB1.

HMGB1 regulates the expression of MHC-I. Following transfection of si-HMGB1 into HaCaT and CaSki cells, the interference efficiency in both cells achieved a 75% gene silencing rate in si-1 (si-HMGB1-1) and si-3 (si-HMGB1-3) transfected groups (Fig. 4A), which was also confirmed by western blotting (Fig. 4B). To confirm the role of HMGB1 knockdown on MHC-I expression, flow cytometry was performed. The MHC-I expression of si-HMGB1-interfered HaCaT cells was reduced after hyperthermia treatment compared with the hyperthermia-treated negative control group (Fig. 4C). HaCaT cell viability assay was performed to confirm the effect of HMGB1 on MHC-I expression was not caused by cytotoxicity (Fig. 4D). Hyperthermia-treated CaSki cells demonstrated downregulated expression of MHC-I compared with the NC

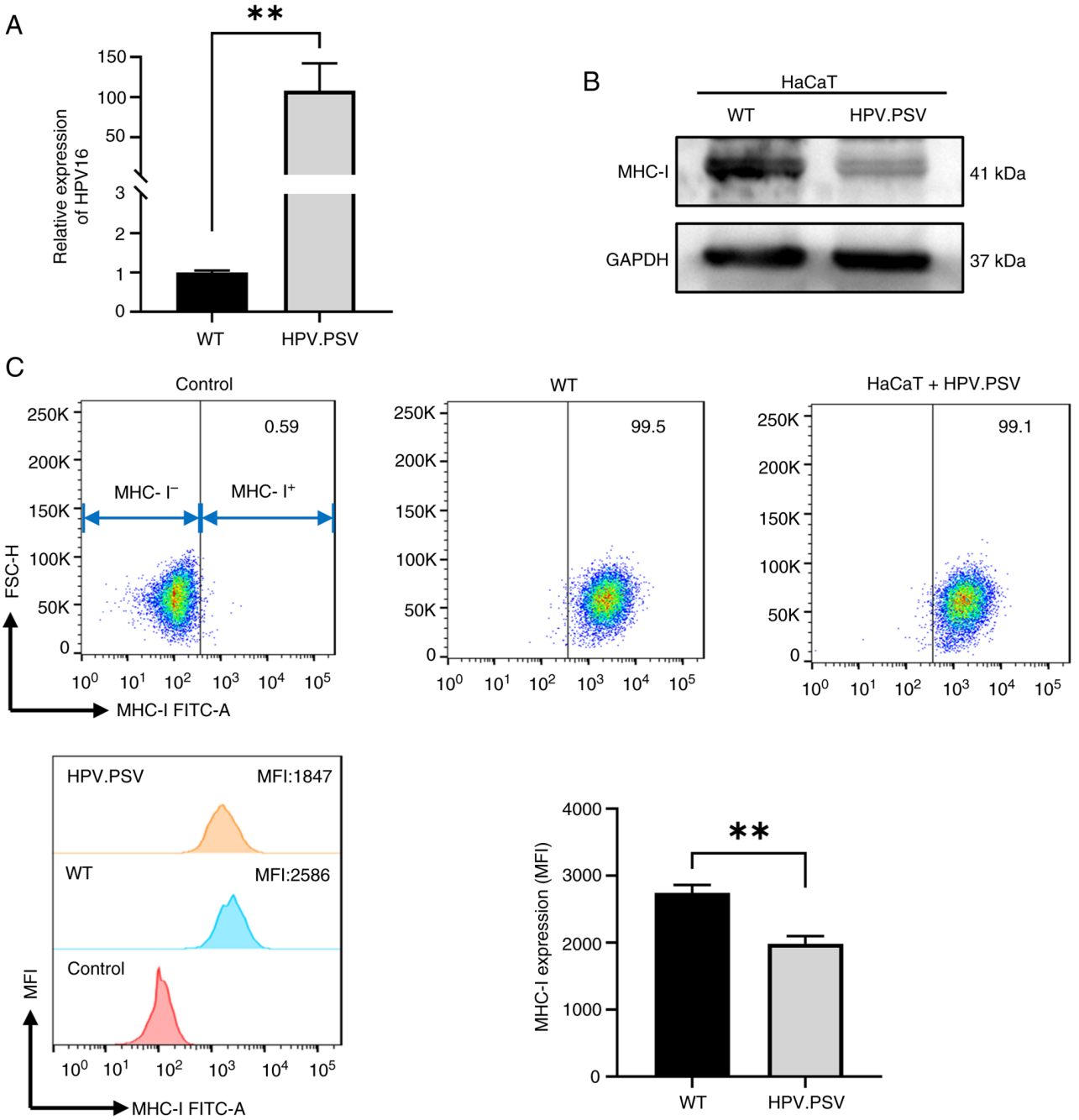

Figure 1. HPV infection decreases the expression of MHC-I. (A) Reverse transcription-quantitative PCR detected the infection efficiency of HPV.PSV. (B) Expression of MHC-I in infected cells was detected by (B) western blotting and (C) flow cytometry. **P<0.01. HPV.PSV, human papillomavirus 16 pseudovirus; MHC-I, major histocompatibility complex class I; WT, wild-type; MFI, mean fluorescence intensity; FSC-H, forward scatter height.

group (Fig. 4E). CaSki cell viability assay was performed to rule out whether the effect of HMGB1 on MHC-I expression was caused by cytotoxicity (Fig. 4F). Furthermore, recombinant HMGB1 protein (rHMGB1) was added to verify the role of HMGB1 in MHC-I expression. Flow cytometry demonstrated that rHMGB1 recovered MHC-I expression in HPV.PSV-infected HaCaT and CaSki cells (Fig. S1A and B). These results complemented the proteomics analysis, confirming the regulatory effect of differentially expressed HMGB1 on immunity. HMGB1 is key for the expression of MHC-I following hyperthermia and HPV infection. To rule out other regulatory molecule, the present study detected the expression of tapasin. During the antigen presentation of MHC-I, peptide loading complex (PLC) serves a key role. Tapasin, as an endoplasmic reticulum chaperone, is a central element of PLC that serves as a molecular chaperone to promote proper folding of MHC-I molecules and loading of antigenic peptides (53). In the present study, hyperthermia did not influence the expression of tapasin (Fig. S2A and B). Therefore, hyperthermia may influence the expression of MHC-I through non-classical antigen-presenting mechanisms.

Hyperthermia-regulated HSPA6 expression influences the secretion of HMGB1 through JNK phosphorylation. Based on our previous findings, HSPA6 expression is significantly induced by hyperthermia treatment (data not been

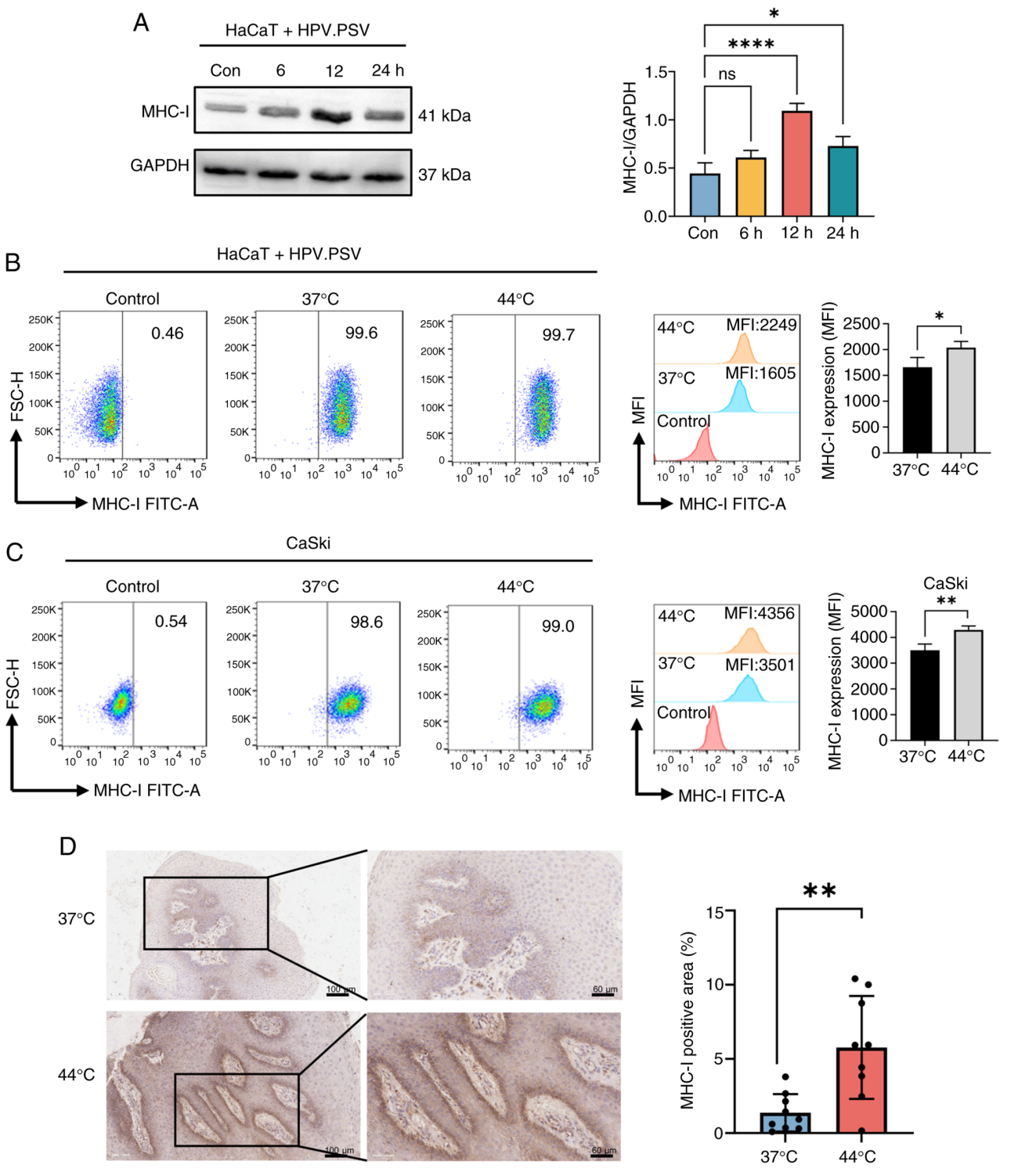

Figure 2. Hyperthermia enhances the expression of MHC-I in HPV-infected cells and condyloma acuminate tissue. Expression of MHC-I in HPV.PSV-infected HaCaT was detected by (A) western blotting and (B) flow cytometry. (C) Flow cytometry was used to detect the expression of MHC-I in CaSki cells. (D) Immunohistochemical staining was used to detect the expression of MHC-I in condyloma acuminate tissue. *P<0.05, **P<0.01, ****P<0.0001. MHC-I, major histocompatibility complex class I; HPV.PSV, HPV 16 pseudovirus; FSC-H, forward scatter height; MFI, mean fluorescence intensity; ns, not significant.

published). Here, HSPA6 was dynamically expressed in HPV.PSV-infected HaCaT and CaSki cells (Fig. 5A). At 4-12 h post-incubation in a 44˚C water bath, HSPA6 presented high expression in both cell lines. Stable cell lines with lentivirus-mediated HSPA6 interference were constructed using sh-HSPA6. Knockdown efficiency was up to 75% in HaCaT and 40% in CaSki cells (Fig. 5B). HSPA6 knockdown notably decreased the expression of HSPA6 and p-JNK in both HPV.PSV-infected HaCaT and CaSki cells following hyperthermia treatment (Fig. 5C). As a member of the HSP70 family, HSPA6 is predicted to participate in JNK phosphorylation (54). HSP70 serves a key role in the protection of dopaminergic neurons by regulating the activation of the JNK pathway (55). The consistent expression of HSPA6

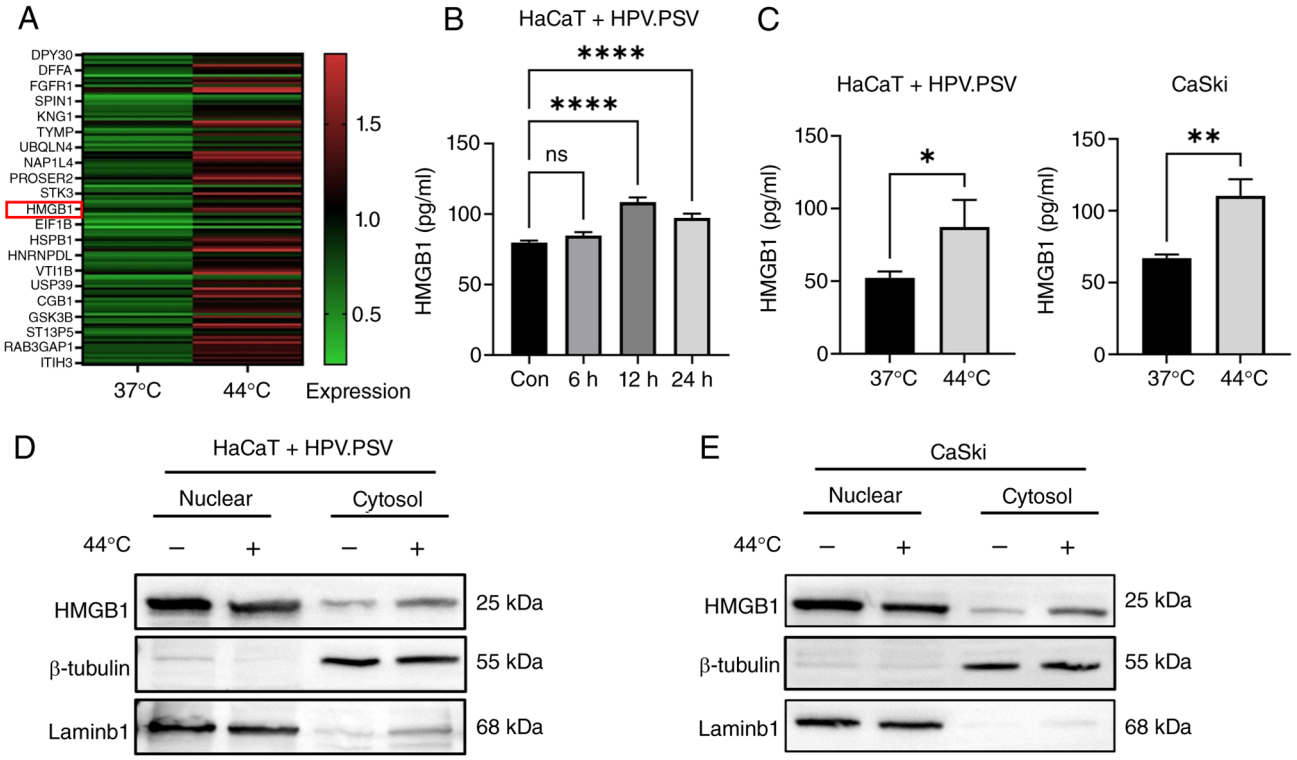

Figure 3. Hyperthermia induces the expression of HMGB1. (A) Heat map of the differentially expressed proteins between 37 and 44˚C-treated CaSki cells by 4D-FastDIA quantitative proteomics. (B) Dynamic secretion of HMGB1 by HPV.PSV-infected HaCaT cells was detected by ELISA post-hyperthermia treatment. (C) ELISA was used to detect the expression of HMGB1 in hyperthermia-treated HPV.PSV-infected HaCaT and CaSki cells. Expression of HMGB1 in nuclear and cytosolic protein was determined by western blotting in HPV.PSV-infected (D) HaCaT and (E) CaSki cells. β-tubulin was used as loading control of cytoplasmic proteins, and Laminb1 as loading control of nuclear proteins. *P<0.05, **P<0.01, ****P<0.0001. HMGB, high mobility group box; HPV.PSV, HPV 16 pseudovirus.

and p-JNK indicated HSPA6 was key for JNK activation. In addition, JNK phosphorylation was upregulated at 12 h post-hyperthermia treatment in HPV.PSV-infected HaCaT cells, as well as 6, 12 and 24 h post-hyperthermia incubation in CaSki cells (Fig. 5D). To study whether HSPA6 directly regulated JNK phosphorylation, Co-IP assay validated the interaction between endogenous HSPA6 and p-JNK in HaCaT and CaSki cells. (Fig. 5E). Finally, to verify the key regulatory molecules, the JNK pathway inhibitor SP600125 and activator anisomycin were applied simultaneously following hyperthermia and secretion of HMGB1 was detected in HPV.PSV-infected HaCaT and CaSki cells. Western blotting analysis revealed that SP600125 significantly suppressed JNK pathway activation at 20 μM in HaCaT cells and at 10 μM in CaSki cells (Fig. S3A and B). Conversely, anisomycin markedly enhanced JNK pathway activation at 0.5 μM in HaCaT cells and at 5 μM in CaSki cells (Fig. S3C and D). JNK activation promoted HMGB1 expression, whereas JNK inhibition suppressed HMGB1 expression in hyperthermia-treated HPV.PSV-infected HaCaT and CaSki cell lines (Fig. 5F). To rule out other regulatory mechanisms regulating HMGB1 secretion, western blotting showed hyperthermia did not influence CRM1 expression in HPV-infected cells (Fig. S4A and B). These results suggested that hyperthermia facilitated HSPA6-modulated JNK phosphorylation, which led to HMGB1 secretion and finally enhanced the expression of MHC-I in HPV-infected epithelial cells, as well as strengthening host immune regulation and recognition.

Discussion

CA is a common sexually transmitted disease caused by HPV infection, which is associated with the escape of host immune surveillance following virus infection. The present study aimed to investigate the regulatory mechanism of hyperthermia treatment on MHC-I expression of HPV-infected epithelial cells. As a key molecule during adaptive immune response, MHC-I presents endogenous antigenic peptides to $CD8^+$ T cells, then activates the CTL response. However, as a highly adapted host virus, HPV has evolved multiple mechanisms to decrease MHC-I expression to evade immune surveillance. HPV16 downregulates MHC-I transcription and surface presentation through histone deacetylase recruitment via its zinc finger domain, and suppresses MHC-I expression by downregulating transporter associated with antigen processing 1 (26,27). Hyperthermia treatment increased the expression of MHC-I in HPV-infected epithelial cells and tissues from patients with CA, which was in accordance with the clinical therapeutic effect of hyperthermia (12). Local hyperthermia alone is effective for genital warts (56). Given its immune-activating effects (T cell infiltration, dendritic cell activation), combining hyperthermia with existing modalities (CO_2 laser, photodynamic therapy) (57) may enhance clearance and decrease recurrence.

Furthermore, 4D-FastDIA quantitative proteomics was performed to analyze the differentially expressed proteins between 37 and 44˚C hyperthermia-treated cells. HMGB1 is a highly conserved nucleoprotein that translocates to the

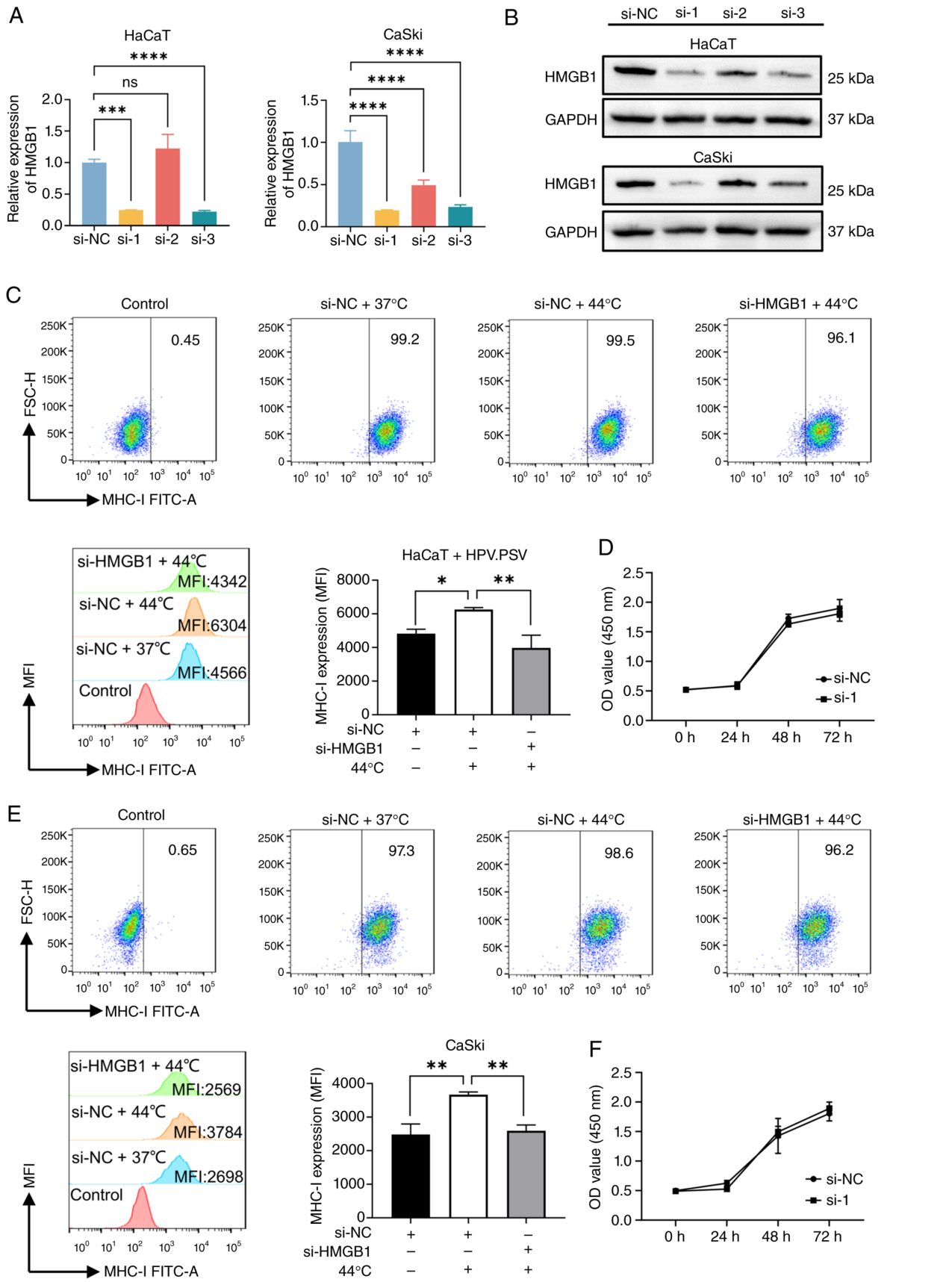

Figure 4. HMGB1 regulates the expression of MHC-I. (A) Reverse transcription-quantitative PCR was performed to detect the si-HMGB1 interference efficiency in HaCaT and CaSki cells. (B) Western blotting was performed to detect the protein levels of HMGB1 after si-HMGB1 interference in HaCaT and CaSki cells. GAPDH was used as loading control. (C) Flow cytometry was performed to detect MHC-I expression. (D) CCK8 assay was performed to detect the HaCaT cell viability following transfection with si-1 or si-NC. (E) Flow cytometry to detect MHC-I expression in si-HMGB1-transfected CaSki cells (F) CCK8 to detect the CaSki cell viability after transfection with si-1 or si-NC. *P<0.05, **P<0.01, ***P<0.001, ****P<0.0001. HMGB, high mobility group box; MHC-I, major histocompatibility complex class I; si, small interfering; CCK8, Cell Counting Kit-8; NC, negative control; FSC-H, forward scatter height; ns, not significant; MFI, mean fluorescence intensity; OD, optical density.

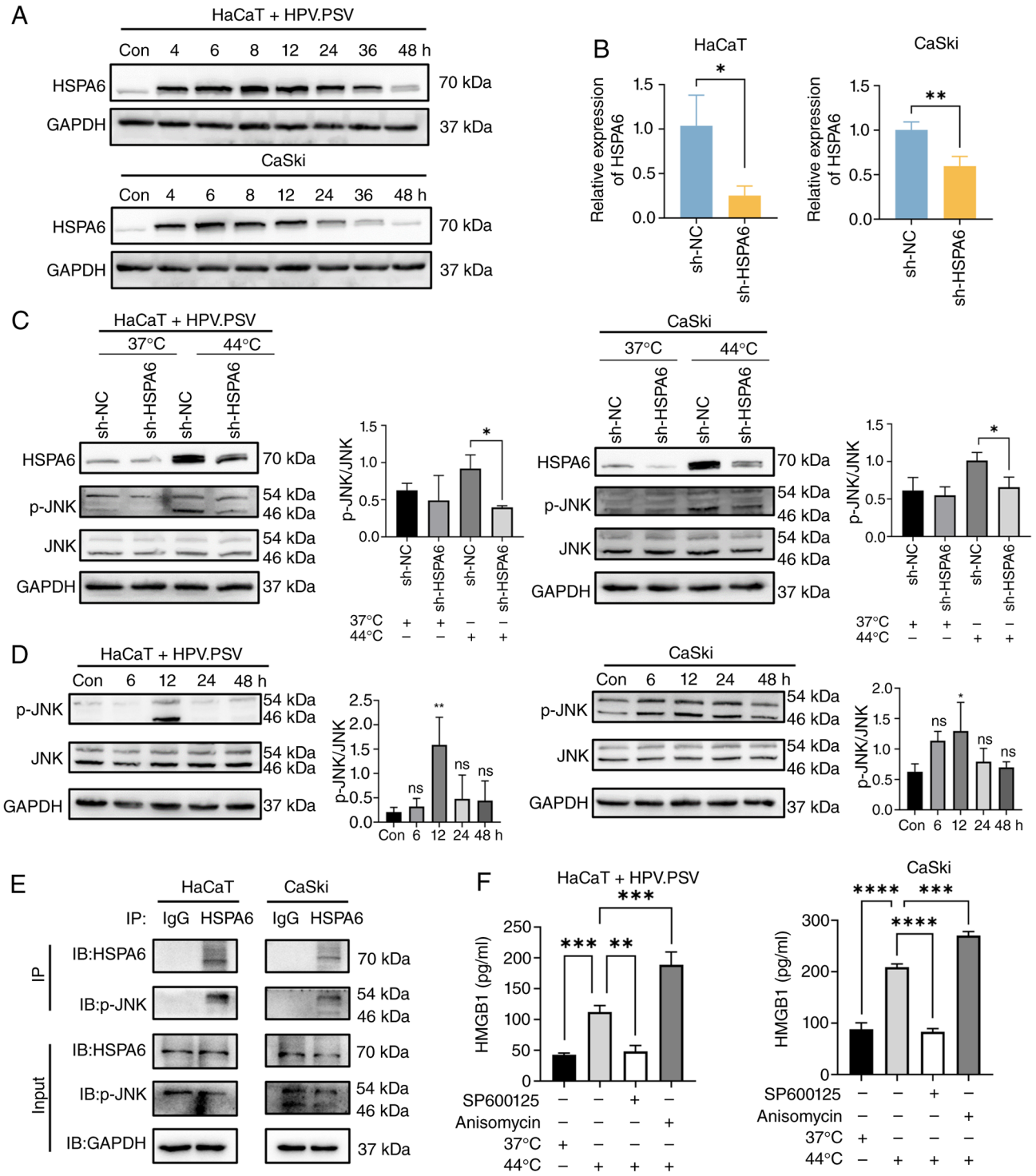

Figure 5. Hyperthermia-regulated HSPA6 expression influences the secretion of HMGB1 through JNK phosphorylation. (A) Western blotting was performed to detect the protein level of HSPA6 in HPV.PSV-infected HaCaT and CaSki cells following hyperthermia treatment. (B) Reverse transcription-quantitative PCR was used to detect the sh-HSPA6 knockdown efficiency in HaCaT and CaSki cells. (C) Western blotting was performed to detect the expression of HSPA6 and JNK/p-JNK. (D) Western blot to detect the expression of JNK/p-JNK. (E) Co-IP was performed to detect the physical binding between HSPA6 and p-JNK in HaCaT and CaSki cells. (F) ELISA was used to detect the secretion of HMGB1 in HPV.PSV-infected HaCaT and CaSki cells stimulated with JNK pathway inhibitor and activator. *P<0.05, **P<0.01, ***P<0.001, ****P<0.0001. HMGB, high mobility group box; HSP, heat shock protein; HPV.PSV, HPV 16 pseudovirus; sh, short hairpin; p-, phosphorylated; IP, immunoprecipitation; Con, control; NC, negative control; ns, not significant; IB, immunoblot.

cytoplasm and is secreted to the extracellular layer under stimulation, including cytokine stimulation and cell death, to function as a DAMP (35,58). HMGB1 participates in the maintenance of chromatin structure under a physiological state and undergoes subcellular redistribution under stress conditions (59). HMGB1, a ligand for pattern recognition receptors including TLR4 and RAGE, activates NF-κB and MAPK, which are important for MHC-I expression (60). The present study confirmed that HMGB1 knockdown reduced the expression of MHC-I.

It is unclear whether hyperthermia modulated HMGB1 expression directly. Based on our previous study (data not published), hyperthermia upregulates expression of HSPA6, which is a member of HSP70 family. HSP70 cross-talks with the MAPK pathway. HSP70 serves a neuro-protective role by regulating the activity of the JNK pathway (55). Hyperthermia induces HSP accumulation and triggers isoform-specific JNK phosphorylation in the rat cerebellum (61). Here, hyperthermia increased HSPA6 expression in a time-dependent manner and loss-of-function experiments demonstrated that HSPA6 regulated JNK phosphorylation directly. HSPA6, as a member of the MAPK signaling pathway family, especially the JNK pathway, is considered to be a key molecular switch regulating HMGB1 secretion under oxidative stress (39). Expression of HMGB1 was regulated by JNK activation. The present study demonstrated that JNK phosphorylation was key for the secretion of HMGB1.

A number of molecular pathways regulate HMGB1 subcellular localization. Acetylation modification mediated by histone acetyltransferase and deacetylase regulates the dynamic distribution of HMGB1 in the karyoplasm (62). HSP90AA1 participates in the nucleoplasmic translocation of HMGB1 and promotes the secretion of HMGB1 through the autophagy polyvesicular pathway (63). To determine other regulatory mechanisms regulating HMGB1 secretion, the present study detected the expression of CRM1, which mediates classical nucleocytoplasmic translocation of HMGB1 (64). Results showed hyperthermia did not influence CRM1 expression in HPV-infected cells which indicated that hyperthermia may regulate the subcellular localization of HMGB1 through other non-classical pathways. The nuclear translocation mechanism of HMGB1 requires further study.

However, there are certain limitations to the present study. There is still no appropriate animal model to mimic HPV infection, which limits the ability to study the immune regulatory mechanism and effect of hyperthermia on CA. The small sample size of the present study (n=9) limits the generalizability of findings. A larger sample size is therefore needed to further evaluate the association between HPV genotype distribution and hyperthermia sensitivity. Future studies with full HPV genotyping and longitudinal follow-up are needed to address genotype-specific responses to hyperthermia treatment. Although the present study focused on the functional role of HMGB1 and MHC-I as secreted/membrane proteins, mRNA expression of HMGB1 and MHC-I should be examined to understand how HMGB1 and MHC-I are regulated by hyperthermia. The involvement of NF-κB also should be explored as HMGB1 is a known DAMP.

In conclusion, hyperthermia treatment facilitated HSPA6-modulated JNK phosphorylation, which led to HMGB1 secretion, enhanced the expression of MHC-I in HPV-infected epithelial cells and strengthened host immune regulation and recognition. The present study established a regulatory axis and potential therapeutic targets for HPV-associated treatment.

Acknowledgements

Not applicable.

Funding

The present study was supported by National Key R&D Program of China (grant no. 2023YFC2508200) and National Natural Science Foundation of China (grant nos. 82173401 and 82373483).

Availability of data and materials

The data generated in the present study may be found in the iProX under accession number IPX0012564000 or at the following URL: iprox.cn/page/home.html.

Authors' contributions

HW performed the experiments. RQQ and TZ designed the experiments and confirm the authenticity of all the raw data. YG and TS analyzed and interpreted data. HL conceived and designed the study. YB analyzed data. All authors read and approved the final manuscript.

Ethics approval and consent to participate

The samples used in the present study were harvested from participants who provided written informed consent, and the procedures were approved by Hospital Medical Science Research Ethics Committee of the First Affiliated Hospital of China Medical University, Shenyang, Liaoning 110122, P.R. China [approval no. (2023)214].

Patient consent for publication

Not applicable.

Competing interests

The authors declare that they have no competing interests.

References

1. Molina MA, Steenbergen RDM, Pumpe A, Kenyon AN and Melchers WJG: HPV integration and cervical cancer: A failed evolutionary viral trait. Trends Mol Med 30: 890-902, 2024.
2. Seliger B, Massa C, Yang B, Bethmann D, Kappler M, Eckert AW and Wickenhauser C: Immune escape mechanisms and their clinical relevance in head and neck squamous cell carcinoma. Int J Mol Sci 21: 7032, 2020.
3. Murray ML, Meadows J, Doré CJ, Copas AJ, Haddow LJ, Lacey C, Jit M, Soldan K, Bennett K, Tetlow M, *et al*: Human papillomavirus infection: Protocol for a randomised controlled trial of imiquimod cream (5%) versus podophyllotoxin cream (0.15%), in combination with quadrivalent human papillomavirus or control vaccination in the treatment and prevention of recurrence of anogenital warts (HIPvac trial). Bmc Med Res Methodol 18: 125, 2018.
4. Stuqui B, Provazzi PJS, Lima MLD, Cabral ÁS, Leonel ECR, Candido NM, Taboga SR, da Silva MG, Lima FO, Melli PPDS, *et al*: Condyloma acuminata: An evaluation of the immune response at cellular and molecular levels. PLoS One 18: e0284296, 2023.
5. Kofoed K, Sand C, Forslund O and Madsen K: Prevalence of human papillomavirus in anal and oral sites among patients with genital warts. Acta Derm Venereol 94: 207-211, 2014.
6. Ye J, Zheng L, He Y and Qi X: Human papillomavirus associated cervical lesion: Pathogenesis and therapeutic interventions. MedComm (2020) 4: e368, 2023.

7. Brown DR, Schroeder JM, Bryan JT, Stoler MH and Fife KH: Detection of multiple human papillomavirus types in Condylomata acuminata lesions from otherwise healthy and immunosuppressed patients. J Clin Microbiol 37: 3316-3322, 1999.
8. Wang J, Chang YZ, Luo H, Jiang W, Xu L, Chen T and Zhu X: Designing immunogenic nanotherapeutics for photothermal-triggered immunotherapy involving reprogramming immunosuppression and activating systemic antitumor responses. Biomaterials 255: 120153, 2020.
9. Mahmood J, Alexander AA, Samanta S, Kamlapurkar S, Singh P, Saeed A, Carrier F, Cao X, Shukla HD and Vujaskovic Z: A combination of radiotherapy, hyperthermia, and immunotherapy inhibits pancreatic tumor growth and prolongs the survival of mice. Cancers (Basel) 12: 1015, 2020.
10. Huo W, Gao YL, Wang HY, Bi GJ, Qiao S, Cai YF, Qi RQ, Yang Y, Lan J, Yao ZR, *et al*: Local hyperthermia versus cryotherapy for treatment of plantar warts: A prospective multi-centre non-randomized concurrent controlled clinical trial. Acta Derm Venereol 102: adv00655, 2022.
11. Sun YZ, Li JF, Wei ZD, Jiang HH, Hong YX, Zheng S, Qi RQ and Gao XH: Proteomic and bioinformatic analysis of condyloma acuminata: Mild hyperthermia treatment reveals compromised HPV infectivity of keratinocytes via regulation of metabolism, differentiation and anti-viral responses. Int J Hyperther 36: 383-393, 2019.
12. Yang Y, Zhang L, Zhang Y, Huo W, Qi R, Guo H, Li X, Wu X, Bai F, Liu K, *et al*: Local hyperthermia at 44˚C is effective in clearing cervical high-risk human papillomaviruses: A proof-of-concept, randomized controlled clinical trial. Clin Infect Dis 73: 1642-1649, 2021.
13. Wei ZD, Sun YZ, Tu CX, Qi RQ, Huo W, Chen HD and Gao XH: DNAJA4 deficiency augments hyperthermia-induced Clusterin and ERK activation: Two critical protective factors of human keratinocytes from hyperthermia-induced injury. J Eur Acad Dermatol Venereol 34: 2308-2317, 2020.
14. Niu X, Zhao Y, Zhang T, Sun Y, Wei Z, Fu K, Li J, Tang M, Wan W, Gao X, *et al*: Comprehensive succinylome analyses reveal that hyperthermia upregulates lysine succinylation of annexin A2 by downregulating sirtuin7 in human keratinocytes. J Transl Int Med 12: 424-436, 2023.
15. Sun YZ, Ren Y, Zhang YJ, Han Y, Yang Y, Gao YL, Zhu LL, Qi RQ, Chen HD and Gao XH: DNAJA4 deficiency enhances NF-kappa B-related growth arrest induced by hyperthermia in human keratinocytes. J Dermatol Sci 91: 256-267, 2018.
16. Han X, Wang HF, Ma L, Chen RX, Wang Q, Zhang CH, Zhang HH, Han Y, Yang Y, Guo H, *et al*: Human papillomavirus genotypes affect the efficacy of hyperthermia therapy for plantar warts: A quality improvement study. J Am Acad Dermatol 93: 536-538, 2025.
17. Jiang F, Shao J, Chen L, Yang N, Liu J and Li Z: Successful treatment of periungual warts with local hyperthermia: Report of two cases. J Dermatolog Treat 33: 2380-2382, 2022.
18. Sengedorj A, Hader M, Heger L, Frey B, Dudziak D, Fietkau R, Ott OJ, Scheidegger S, Barba SM, Gaipl US and Rückert M: The effect of hyperthermia and radiotherapy sequence on cancer cell death and the immune phenotype of breast cancer cells. Cancers (Basel) 14: 2050, 2022.
19. Chen O, Michlíková S, Eckhardt L, Wondrak M, De Mendoza AM, Krause M, McLeod DD and Kunz-Schughart LA: Efficient heat shock response affects hyperthermia-induced radiosensitization in a tumor spheroid control probability assay. Cancers (Basel) 13: 3168, 2021.
20. Wang X, Gao XH, Hong Y, Li X and Chen HD: Local hyperthermia decreases the expression of CCL-20 in condyloma acuminatum. Virol J 7: 301, 2010.
21. Wang GH, Wang YB, Cheng YA, Chen HD, Gao XH and Qi RQ: Local hyperthermia combined with imiquimod cleared recalcitrant and extensive warts in a patient with systemic lupus erythematosus. Clin Cosmet Investig Dermatol 18: 241-244, 2025.
22. Tu YC, Yeh WC, Fang YW, Lo KH, Liang LN, Liu XC, Tsai CC, Cheng CC, Lin MC, Yu HH and Su BC: Hyperthermia-induced cytotoxicity and modulation of PD-L1 and MHC-I expression in human non-small cell lung cancer cell lines. Exp Physiol: Jul 8, 2025 (Epub ahead of print).
23. Wang X, Waschke BC, Woolaver RA, Chen SMY, Chen Z and Wang JH: MHC class I-independent activation of virtual memory CD8 T cells induced by chemotherapeutic agent-treated cancer cells. Cell Mol Immunol 18: 723-734, 2021.
24. Tobian AAR, Canaday DH, Boom WH and Harding CV: Bacterial heat shock proteins promote CD91-dependent class I MHC cross-presentation of chaperoned peptide to CD8+ T cells by cytosolic mechanisms in dendritic cells versus vacuolar mechanisms in macrophages. J Immunol 172: 5277-5286, 2004.
25. Wooldridge L, Lissina A, Vernazza J, Gostick E, Laugel B, Hutchinson SL, Mirza F, Dunbar PR, Boulter JM, Glick M, *et al*: Enhanced immunogenicity of CTL antigens through mutation of the CD8 binding MHC class I invariant region. Eur J Immunol 37: 1323-1333, 2007.
26. Heller C, Weisser T, Mueller-Schickert A, Rufer E, Hoh A, Leonhardt RM and Knittler MR: Identification of key amino acid residues that determine the ability of high risk HPV16-E7 to dysregulate major histocompatibility complex class I expression. J Biol Chem 286: 10983-10997, 2011.
27. Deng XM, Li W, Zhang X, Wang CX, Dong ZG, Zhang X, Zheng GX, Zhang XH, Zheng N, Wang LL, *et al*: RNA interference of human papillomavirus type 16 E7 increases HLA class I antigen expression in HaCaT-E7 cells. Int J Gynecol Cancer 21: 28-34, 2011.
28. Taylor BC and Balko JM: Mechanisms of MHC-I downregulation and role in immunotherapy response. Front Immunol 13: 844866, 2022.
29. Westrich JA, Vermeer DW, Silva A, Bonney S, Berger JN, Cicchini L, Greer RO, Song JI, Raben D, Slansky JE, *et al*: CXCL14 suppresses human papillomavirus-associated head and neck cancer through antigen-specific $CD8^+$ T-cell responses by upregulating MHC-I expression. Oncogene 38: 7166-7180, 2019.
30. Pang X, Zhang Y, Wei H, Zhang J, Luo Q, Huang C and Zhang S: Expression and effects of high-mobility group box 1 in cervical cancer. Int J Mol Sci 15: 8699-8712, 2014.
31. Guo L, Wang D, Jiang X and He G: HMGB1: From molecular functions to clinical applications in cancer and inflammatory diseases. Med Res Rev 46: 408-444, 2026.
32. Wang S and Zhang Y: HMGB1 in inflammation and cancer. J Hematol Oncol 13: 116, 2020.
33. Dong H, Zhang L and Liu S: Targeting HMGB1: An available therapeutic strategy for breast cancer therapy. Int J Biol Sci 18: 3421-3434, 2022.
34. Yang HM, Zhao XN, Li XL, Wang X, Pu Y, Wei DK and Li Z: A pan-cancer analysis of the oncogenic function of HMGB1 in human tumors. Biochem Biophys Rep 40: 101851, 2024.
35. Sims GP, Rowe DC, Rietdijk ST, Herbst R and Coyle AJ: HMGB1 and RAGE in inflammation and cancer. Annu Rev Immunol 28: 367-388, 2010.
36. Luo Y, Li SJ, Yang J, Qiu YZ and Chen FP: HMGB1 induces an inflammatory response in endothelial cells via the RAGE-dependent endoplasmic reticulum stress pathway. Biochem Biophys Res Commun 438: 732-738, 2013.
37. Tang YT, Zhao X, Antoine D, Xiao X, Wang H, Andersson U, Billiar TR, Tracey KJ and Lu B: Regulation of posttranslational modifications of HMGB1 during immune responses. Antioxid Redox Sign 24: 620-634, 2016.
38. Bianchi ME, Crippa MP, Manfredi AA, Mezzapelle R, Rovere Querini P and Venereau E: High-mobility group box 1 protein orchestrates responses to tissue damage via inflammation, innate and adaptive immunity, and tissue repair. Immunol Rev 280: 74-82, 2017.
39. Tang D, Shi Y, Kang R, Li T, Xiao W, Wang H and Xiao X: Hydrogen peroxide stimulates macrophages and monocytes to actively release HMGB1. J Leukocyte Biol 81: 741-747, 2007.
40. Grundtman C, Bruton J, Yamada T, Ostberg T, Pisetsky DS, Harris HE, Andersson U, Lundberg IE and Westerblad H: Effects of HMGB1 on in vitro responses of isolated muscle fibers and functional aspects in skeletal muscles of idiopathic inflammatory myopathies. FASEB J 24: 570-578, 2010.
41. Wan Z, Zhang X, Peng A, He M, Lei Z and Wang Y: TLR4-HMGB1 signaling pathway affects the inflammatory reaction of autoimmune myositis by regulating MHC-I. Int Immunopharmacol 41: 74-81, 2016.
42. Li Z, Deng J, Sun J and Ma Y: Hyperthermia targeting the tumor microenvironment facilitates immune checkpoint inhibitors. Front Immunol 11: 595207, 2020.
43. Zhao W, An H, Zhou J, Xu H, Yu Y and Cao X: Hyperthermia differentially regulates TLR4 and TLR2-mediated innate immune response. Immunol Lett 108: 137-142, 2007.
44. Wang L, Fu H, Zhao J, Liu Z, Chen S, Zhang CQ, Hu P, Wang J, Shi J and Jia W: Cascade magnetic hyperthermia therapy for biofilm eradication and bone regeneration via dual osteoimmuno-regulation. ACS Nano 19: 21679-21695, 2025.

45. Anbar M: Hyperthermia of the cancerous breast: Analysis of mechanism. Cancer Lett 84: 23-29, 1994.
46. Teicher BA, Holden SA, Liu CJ, Ara G and Herman TS: Minocycline as a modulator of chemotherapy and hyperthermia in vitro and in vivo. Cancer Lett 82: 17-25, 1994.
47. Demichev V, Messner CB, Vernardis SI, Lilley KS and Ralser M: DIA-NN: Neural networks and interference correction enable deep proteome coverage in high throughput. Nat Methods 17: 41-44, 2020.
48. Livak KJ and Schmittgen TD: Analysis of relative gene expression data using real-time quantitative PCR and the 2(-Delta Delta C(T)) method. Methods 25: 402-408, 2001.
49. Janke C and Bulinski JC: Post-translational regulation of the microtubule cytoskeleton: mechanisms and functions. Nat Rev Mol Cell Bio 12: 773-786, 2011.
50. Dechat T, Pfleghaar K, Sengupta K, Shimi T, Shumaker DK, Solimando L and Goldman RD: Nuclear lamins: Major factors in the structural organization and function of the nucleus and chromatin. Gene Dev 22: 832-853, 2008.
51. Zhong H, Li X, Zhou S, Jiang P, Liu X, Ouyang M, Nie Y, Chen X, Zhang L, Liu Y, *et al*: Interplay between RAGE and TLR4 regulates HMGB1-induced inflammation by promoting cell surface expression of RAGE and TLR4. J Immunol 205: 767-775, 2020.
52. Gillespie KP, Pirnie R, Mesaros C and Blair IA: Cisplatin dependent secretion of immunomodulatory high mobility group box 1 (HMGB1) protein from lung cancer cells. Biomolecules 13: 1335, 2023.
53. Boulanger DSM, Douglas LR, Duriez PJ, Kang Y, Dalchau N, James E and Elliott T: Tapasin-mediated editing of the MHC I immunopeptidome is epitope specific and dependent on peptide off-rate, abundance, and level of tapasin expression. Front Immunol 13: 956603, 2022.
54. Wang SH, Jiang JX, Zheng KT, Zhang SJ, Chen TD and Wang Z: Exosome-derived Menin from cancer-associated fibroblasts promotes gastric cancer progression by activating the HSPA6/JNK/JunD pathway and inducing EMT. J Transl Med 24: 274, 2025.
55. Shukla AK, Pragya P, Chaouhan HS, Tiwari AK, Patel DK, Abdin MZ and Chowdhuri DK: Heat shock protein-70 (Hsp-70) suppresses paraquat-induced neurodegeneration by inhibiting JNK and caspase-3 activation in Drosophila model of Parkinson's disease. PLoS One 9: e98886, 2014.
56. Piguet V: Heat-induced editing of HPV genes to clear mucocutaneous warts? J Invest Dermatol 137: 796-797, 2017.
57. Scheinfeld N: Update on the treatment of genital warts. Dermatol Online J 19: 18559, 2013.
58. Papatheodorou A, Stein A, Bank M, Sison CP, Gibbs K, Davies P and Bloom O: High-mobility group box 1 (HMGB1) is elevated systemically in persons with acute or chronic traumatic spinal cord injury. J Neurotraum 34: 746-754, 2017.
59. Zhao G, Fu C, Wang L, Zhu L, Yan Y, Xiang Y, Zheng F, Gong F, Chen S and Chen G: Down-regulation of nuclear HMGB1 reduces ischemia-induced HMGB1 translocation and release and protects against liver ischemia-reperfusion injury. Sci Rep 7: 46272, 2017.
60. Zhang Z, Ji R, Liu Z, Jiang Z, Chu M, Wang Y and Zhao J: hUMSC-Exosomes suppress TREM1-p38 MAPK signaling via HMGB1-dependent mechanisms to reprogram microglial function and promote neuroprotection in ischemic stroke. J Nanobiotechnology 23: 572, 2025.
61. Schiaffonati L, Maroni P, Bendinelli P, Tiberio L and Piccoletti R: Hyperthermia induces gene expression of heat shock protein 70 and phosphorylation of mitogen activated protein kinases in the rat cerebellum. Neurosci Lett 312: 75-78, 2001.
62. Chen RC, Kang R and Tang DL: The mechanism of HMGB1 secretion and release. Exp Mol Med 54: 91-102, 2022.
63. Kim YH, Kwak MS, Lee B, Shin JM, Aum S, Park IH, Lee MG and Shin JS: Secretory autophagy machinery and vesicular trafficking are involved in HMGB1 secretion. Autophagy 17: 2345-2362, 2021.
64. Fukuda M, Asano S, Nakamura T, Adachi M, Yoshida M, Yanagida M and Nishida E: CRM1 is responsible for intracellular transport mediated by the nuclear export signal. Nature 390: 308-311, 1997.